Seismic noise level variation in South Korea

Dong-Hoon Sheen*⎫ *Earthquake Research Center, Geological Research Division, Korea Institute of Geoscience and Min-*
Jin Soo Shin   ⎭ *eral Resources, Daejeon 305-350, Korea*
Tae-Seob Kang   *Department of Environmental Geosciences, Pukyong National University, Busan 608-737, Korea*

ABSTRACT: Variations of seismic background noise in South Korea have been investigated using power spectral analysis. We have estimated the power spectral density of seismic noise for 30 broadband stations from 2005 to 2007. In the frequency range 1–5 Hz, diurnal variations of noise level and daily differences in daytime noise level are observed at most stations, suggesting that cultural activities contribute to the noise level of a station. The variation in the number of stations detecting an event, however, suggests that cultural noise has little influence on the detection capability of events over magnitude 2.0. In the frequency range 0.1–0.5 Hz, a double-frequency (DF) peak is dominant at all stations. Clear seasonal variations of peaks are observed, while much less shown in the frequency range 1–5 Hz. DF noise levels are higher in winter than in summer. Strong DF peaks occur in summer when Pacific typhoons near the Korean Peninsula. The discrepancy in time between DF peaks at seismic stations and peaks of significant wave height at buoys, as well as the decrease of DF peaks with increased latitude, indicate that the likely source region of DF peaks is located in the Southern Sea of Korea.

Key words: seismic background noise, diurnal variation, seasonal variation, double frequency microseism

1. INTRODUCTION

The earth is dynamic. Background seismic noise is therefore unavoidable in seismic data and varies temporally and spatially. Analysis of seismic noise can improve our understanding of the Earth system, providing insight into such processes as atmosphere-ocean-seafloor coupling (Rhie and Romanowicz, 2004). Seismic noise analysis is also important to consider for the operation of seismic networks because variations in the seismic noise level may have a significant effect on the detection capability of a seismic network.

Numerous studies have examined seismic noise. At frequencies higher than 1 Hz, cultural noise and wind turbulence are the principal causes of noise (Young et al., 1996; Withers et al., 1996), but borehole seismometers can significantly improve high-frequency signal-to-noise ratios (Aster and Shearer, 1991; Carter et al., 1991). Ringdal and Bungum (1977) reported that no measurable diurnal fluctuation in event detectability had been observed but the false alarm rate of automatic Norwegian Seismic Array (NORSAR) event

detectors increased at night, which was explained by the superimposition of the diurnal variation of the cultural noise level on the background seismic noise field. This means that instantaneous noise peaks that cause detections are insignificant and are determined to be false alarms. Marzorati and Bindi (2006) showed that a high noise level could limit the detection of weak earthquakes by synthetic tests that estimate the spatial variability of detection thresholds of the seismic network.

In the frequency range 0.1–0.5 Hz, a strong peak has been well observed throughout the world. Known as the secondary microseism or double-frequency (DF) peak, this peak has a frequency twice as large as that of oceanic waves. Longuet-Higgins (1950) explained that the DF peak is generated by a pressure excitation at the ocean floor due to the interaction of opposing oceanic waves of the same frequency traveling in opposite directions. Many studies have reported the conditions giving rise to DF peak generation and the relationship between storms and DF peak (Friedrich et al., 1998; Schulte-Pelkum et al., 2004; Bromirski et al., 2005; Chevrot et al., 2007; Kedar et al., 2008).

The primary microseism is observed in the 0.05–0.1 Hz frequency range; these frequencies are the same as those of ocean swells directly interacting with the shallow seafloor and of ocean waves (Hasselmann, 1963).

In this study, we have analyzed the background seismic noise level in South Korea and studied the diurnal and seasonal variations of this noise in the frequency ranges 1–5 and 0.1–0.5 Hz. The primary microseism range is also briefly discussed. To evaluate the power spectral density of seismic noise, we apply the method proposed by McNamara and Buland (2004) to seismograms recorded at 30 broadband stations from 2005 to 2007.

2. DATA AND METHOD

Several institutions now operate broadband seismic networks in South Korea. The Korea Institute of Geoscience and Mineral Resources (KIGAM) and the Korea Meteorological Administration (KMA) have nationwide seismic networks, while other seismic networks are operated around some specific properties, such as power plants. Therefore,
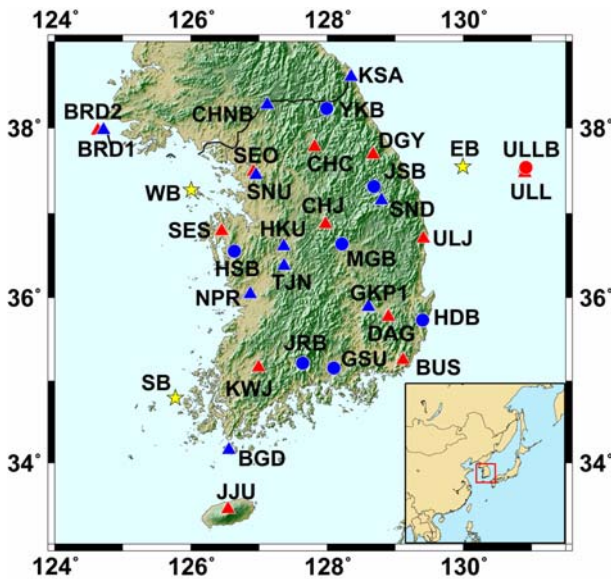

Fig. 1. Seismic networks in South Korea in 2007. Blue and Red represent the KIGAM and KMA networks, respectively. Triangles indicate STS-2 sensor and circles indicate CMG-3TB. Yellow stars indicate buoys.

we use seismograms from the KIGAM and KMA networks to investigate the background seismic noise level in South Korea.

As of the end of 2007, there were 30 broadband stations that had been operating for more than 1 year, 17 operated by KIGAM and 13 operated by the KMA. Figure 1 shows the locations of all the stations examined in this study. The mechanical conditions are similar at all stations, but local site conditions differ from site to site. All stations but eight are equipped with three-component Streckeisen STS-2 sensors. The eight remaining stations have boreholes equipped with Guralp CMG-3TB sensors. All borehole sensors are installed at about 60-m depth, except for one (ULLB), which is installed at 100-m depth. Table 1 shows the location and elevation of the stations and describes each site in terms of sensor type.

To estimate the power spectral density (PSD) of the seismic noise, we have used a large number of 1-day-long continuous seismograms from 2005 to 2007, each with a sampling rate of 20 sps. Stations JRB, JSB, and YKB of KIGAM, and ULLB of the KMA were installed at the end of 2006. Because of archiving problems, most of the KMA data from September 2005 to April 2006 cannot be used, and the data from station ULLB is usable only from March 2007.

To estimate PSDs from thousands of continuous time series, we use the robust PSD estimation method of McNamara and Buland (2004). An advantage of this method is that it does not require a quiet time window during the day in order to avoid the effects of earthquakes or instrumental malfunctions. However, we carefully excluded 1-day-long seismograms that showed systematic glitches of more than

2 hours, even though these artifacts would have had little effect on the overall noise levels of a station.

For the spectral analysis, each 1-day-long continuous seismogram is parsed into 1- hour segments, with 50% overlap, and distributed continuously in time. To improve the fast Fourier transform (FFT) speed, the number of samples in the seismogram is truncated to the next lowest power of two. To reduce variance in the PSD estimate, each 1-hour time series seismogram is divided into 13 segments, overlapping by 75%. Then, the mean and long-period linear trend are removed. After applying a 10% cosine taper to reduce spectral leakage, the spectrum of each segment is computed by the FFT algorithm. Finally, instrument response is removed, and the PSD estimate is converted into decibels (dB) with respect to acceleration $(m/s^2)^2/Hz$.

The probability density function (PDF) of the PSD estimates is constructed to investigate the noise level at a given station. For every 1-hour PSD estimate, spectral powers are accumulated in 1-dB bins for each period. The probability of occurrence of a given power at a particular period can then be estimated. In this study, we use the mode of PDFs to describe the noise level at a given station.

3. RESULTS AND DISCUSSION

Figure 2 shows the PDFs for three components, east-west (E), north-south (N), and vertical (Z), at station HSB where seismograms were recorded from 2005 to 2007. The color represents the probability of noise level at a given period. The upper and lower solid curves are the high and low noise models given by Peterson (1993). The dashed lines represent the statistical mode of the PDF, which represents the highest probability noise level of a given channel of a station. We computed the PDFs for the other stations in the same manner.

Seismic noise levels show considerable diurnal variations in frequencies higher than 1 Hz. On the other hand, the noise levels in the frequency range 0.1–0.5 Hz does not exhibit notable diurnal variations similar to those at high frequencies (>1 Hz); however, they show systematic seasonal variations, which will be discussed later. Noise levels during daytime and nighttime are measured by averaging the modes in the frequency range 1–5 Hz for local daytime (6–18 h) and nighttime (0–6 h and 18–24 h), respectively. Diurnal variation of noise level is observed at most stations and even at boreholes, although the amplitude varies by station and period. Daytime noise levels are approximately 4 dB above nighttime levels. Noise level variations of horizontal components and those of vertical components are measured similarly at each station. Figure 3 shows noise levels of the vertical component at nighttime, denoted by the color of circles, and noise level differences between daytime and nighttime, denoted by the size of circles. High noise levels are observed at the stations located in large cities

Table 1. Station descriptions

Code	Network	Latitude	Longitude	Elevation (m)	Sensor
BGD	KIGAM	34.1569	126.5575	6	STS-2
BRD*	KIGAM	37.9771	124.7142	78	STS-2
BRD*	KMA	37.9677	124.6303	169	STS-2
BUS	KMA	35.2487	129.1125	91	STS-2
CHC	KMA	37.7775	127.8145	245	STS-2
CHJ	KMA	36.8730	127.9748	227	STS-2
CHNB	KIGAM	38.2685	127.1185	176	STS-2
DAG	KMA	35.7685	128.8970	262	STS-2
DGY	KMA	37.6904	128.6742	791	STS-2
GKP1	KIGAM	35.8893	128.6056	47	STS-2
GSU	KIGAM	35.1520	128.0990	35 (60)	CMG-3TB
HDB	KIGAM	35.7307	129.4012	145(60)	CMG-3TB
HKU	KIGAM	36.6101	127.3602	67	STS-2
HSB	KIGAM	36.5525	126.6380	53 (60)	CMG-3TB
JJU	KMA	33.4306	126.5463	542	STS-2
JRB	KIGAM	35.2100	127.6425	75 (66)	CMG-3TB
JSB	KIGAM	37.3146	128.6876	316 (65)	CMG-3TB
KSA	KIGAM	38.5926	128.3538	103	STS-2
KWJ	KMA	35.1599	126.9910	213	STS-2
MGB	KIGAM	36.6373	128.2169	108 (62)	CMG-3TB
NPR	KIGAM	36.0395	126.8685	19	STS-2
SES	KMA	36.7893	126.4531	99	STS-2
SEO	KMA	37.4879	126.9188	33	STS-2
SND	KIGAM	37.1549	128.7984	756	STS-2
SNU	KIGAM	37.4509	126.9566	161	STS-2
TJN	KIGAM	36.3775	127.3638	52	STS-2
ULJ	KMA	36.7021	129.4084	77	STS-2
ULL	KMA	37.4736	130.9008	218	STS-2
ULLB	KMA	37.5406	130.9169	5 (100)	CMG-3TB
YKB	KIGAM	38.2253	127.9902	260 (62)	CMG-3TB

*KIGAM and KMA used the same code name; thus for this study we used the codes BRD1 and BRD2, respectively. Numbers in parentheses refer to the depth of the borehole.
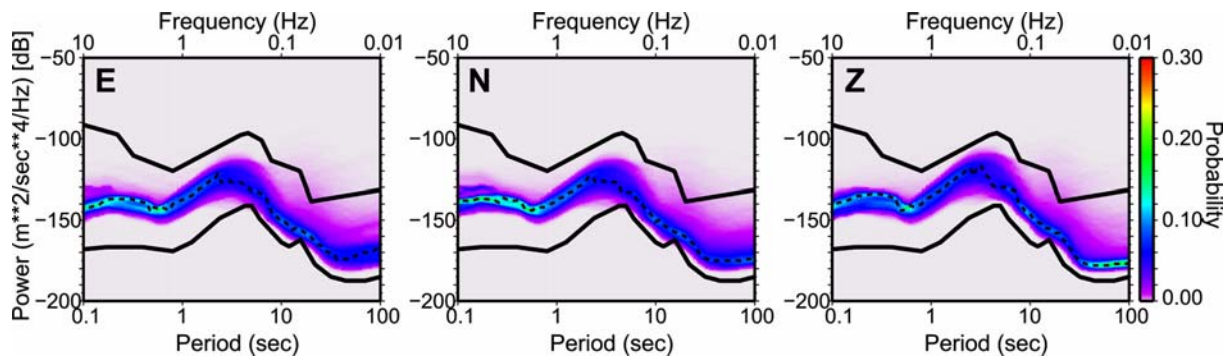

Fig. 2. PDFs for station HSB estimated using data from 2005 to 2007. The upper and lower solid lines are the high and low noise models of Peterson (1993), and the dashed lines are the statistical mode. E, N, and Z represent east-west, north-south, and vertical components, respectively.

(SEO, GSU, GKP1, SNU, BUS, HKU, and TJN) and at island stations (ULL, ULLB, JJU, BRD1, and BRD2). Station JJU shows the largest variation (13.73 dB), while station CHJ has the smallest variation (1.15 dB).

Figure 4 presents the daily difference in the daytime noise level of the vertical component. The horizontal components show similar features. Daytime noise levels of each station are averaged over all days, and their means are subtracted
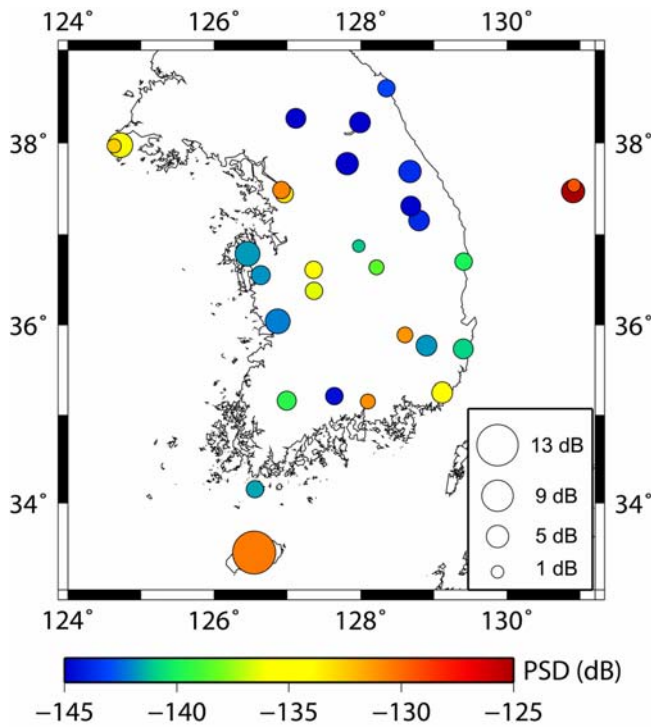
Fig. 3. Nighttime noise levels of vertical component and noise level differences between daytime and nighttime in the frequency range 1–5 Hz. Colors denote noise level, and the size of circle represents the difference.

from each daily noise level. Daily difference is observed at most stations in South Korea, with Sunday noise level being lower than noise levels on other days. The differences at the eight stations (BUS, CHJ, DAG, GKP1, GSU, SEO, SNU, and TJN) located in urban areas are more than 2 dB, while the differences at the five stations (BGD, BRD1, BRD2, KSA, and ULL) in rural areas are quite low (less than
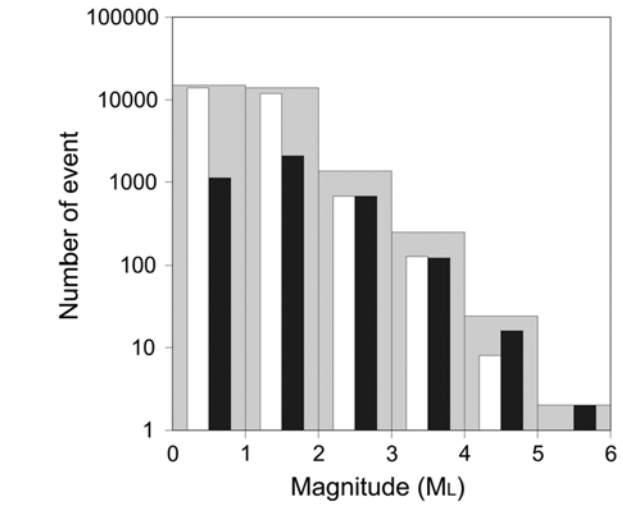

Fig. 5. Number of events reported by KIGAM's earthquake monitoring system versus magnitude. Gray, white and black bars represent number of events occurring during whole day, daytime and nighttime, respectively.

1 dB). In particular, station ULLB does not exhibit daily differences in noise levels. This station, situated on a scenic volcanic island, seems to be noisier on weekends than on weekdays. It is noteworthy that the noise level of Sunday daytime is very close to that of nighttime at all stations except for station ULLB. This suggests that cultural noises are the dominant factor contributing to the diurnal variation.

To discuss the effect of the diurnal variation of noise levels on the detection capability of the seismic network, we examine the event detection history of KIGAM's earthquake monitoring system, which includes records of stations reporting individual seismic events. Figure 5 shows the number of events as a function of magnitude. Colors of bars correspond to the origin time of the earthquake. Gray
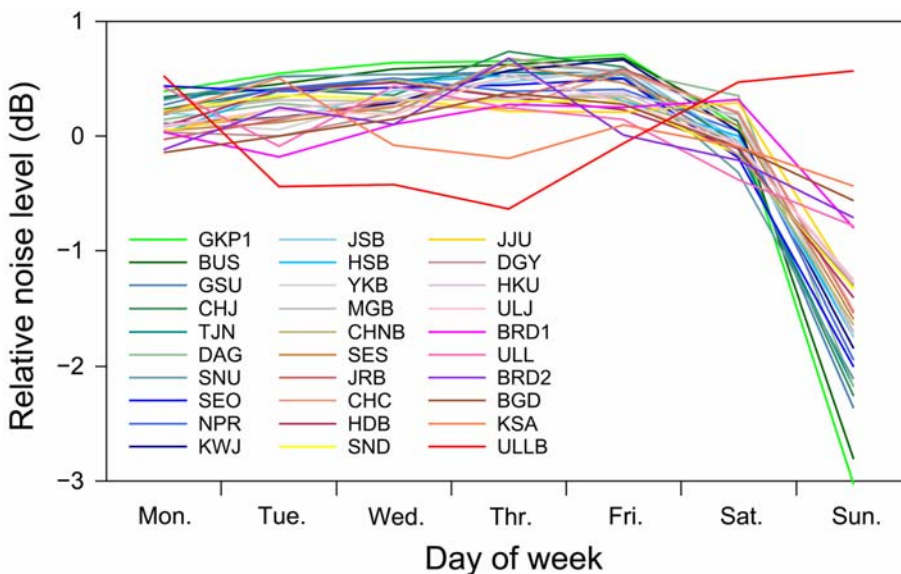

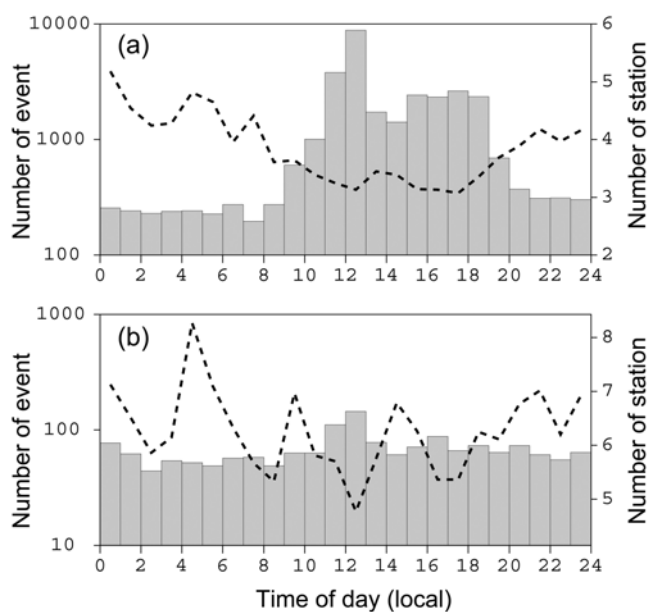**Fig. 4.** Daily difference of daytime noise level of the vertical component.

Fig. 6. Number of KIGAM-reported events (histogram) and number of stations reporting local magnitude (dashed line). (a) all event and (b) events whose magnitude greater than 2.0. The data cover the time period 2001–2007.

bar indicates the total number of events while white and black bars indicate the numbers of events occurring during daytime and nighttime, respectively. It is clear that the events less magnitude 2.0 occurred more during daytime than nighttime.

Figure 6 shows the diurnal distribution of the number of events from 2001 to 2007, and that of stations where local magnitudes are measured. The histograms correspond to the number of events, while the dashed lines correspond to the number of stations. The upper and lower figures show distributions of all event and events over magnitude 2.0, respectively. Figure 6a also shows that most events have been occurred during the daytime. However, the magnitudes of almost all events during the daytime are lower than 2.0 (see Fig. 5), indicating that the sources of these events would have been artificial sources, such as explosions and quarry blasts. Not that all artificial explosions after sunset are prohibited in South Korea. It is also shown that the number of stations reporting local magnitudes decreases by up to three during the daytime, but increases by up to five during the nighttime. Small events can be identified only at stations close to the epicenter, which would depend on the station density of the network, because seismic energy from small
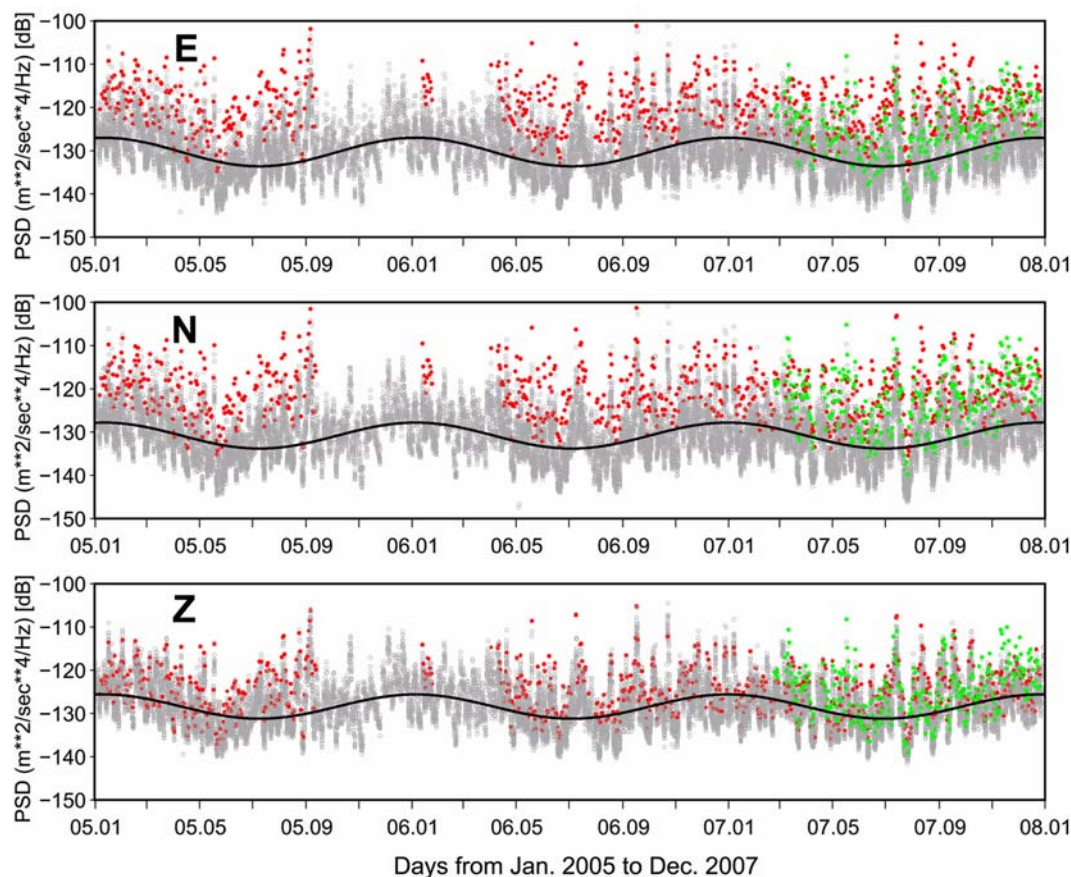

Fig. 7. Seasonal variations of the DF peak at all stations used in this study from 2005 to 2007. E, N, and Z represent east-west, north-south, and vertical components, respectively. Gray dots represent noise levels of individual stations, and red and green dots represent stations JJU and ULLB, respectively.

events attenuates within distances of several tens of kilo-meters. Consequently, the number of stations detecting indi-vidual events is smaller in daytime when large numbers of small artificial explosions occurs. On the other hand, the number of events having magnitudes greater than 2.0 shows a uniform distribution overall, irrespective of time of day, and the number of stations shows a random distribution (Fig. 6b). Since the diurnal variation of the noise level is not correlated with the event detection history over magnitude 2.0, we conclude that cultural noise has little influence on the detection capability of events above this magnitude threshold in KIGAM's seismic network.

The DF peak is dominant for seismic noise in the fre-quency range 0.1–0.5 Hz (see Fig. 2). To emphasize the sea-sonal variation of the DF peak, the daily noise level is estimated by averaging the modes in the range 0.1–0.5 Hz. Figure 7 shows the seasonal variation at all stations in the DF range. Gray dots represent daily noise levels at each station, and red and green dots indicate those levels at stations JJU and ULLB, respectively. Black lines are the sine functions of best fit. Seasonal variation is clearly observed at all stations, and noise levels are higher in the winter than in the summer. Seasonal variation in the primary microseism range is also observed similarly, but smaller (3.5 dB) than in the DF range (6.1 dB).

The noise level and its variations are almost the same for all three components (Fig. 7). However, stations JJU and ULLB, both installed at volcanic islands, have higher noise levels for horizontal components than for vertical compo-nents. Similar observations are reported for the coastal zone of the Kamchatka east coast (Gordeev, 1990). In general, the DF microseism is thought to be produced by the vertical interaction with the changing potential energy of ocean waves and to travel as Rayleigh waves (Haubrich and McCamy, 1969; Barstow et al., 1989). The conversion of Rayleigh waves to Love waves during propagation has been suggested to explain the generation of shear components of microseisms. However, these explanations do not sufficiently explain the generation of horizontal microseisms that are greater than the vertical microseisms. Therefore, it is likely that some of horizontal energy also results from bottom friction (Gordeev, 1990), or from the same pressure force responsible for gen-erating Rayleigh waves acting on an inclined surface (Rind and Donn, 1979). The steep bathymetry of the small vol-canic islands at which stations JJU and ULLB are located may add support to the suggested explanations of Rind and Donn (1979).

Several strong peaks are notable in the summer. The DF peak is known to depend on the amplitude of ocean waves and the location of the generation region (Longuet-Higgins, 1950; Bromirski et al., 2005; Kedar et al., 2008). Figure 8 illustrates the correlation between the DF peak and an ocean storm; the variation of the PSDs of vertical compo-nents in summer 2006 is plotted with the significant wave
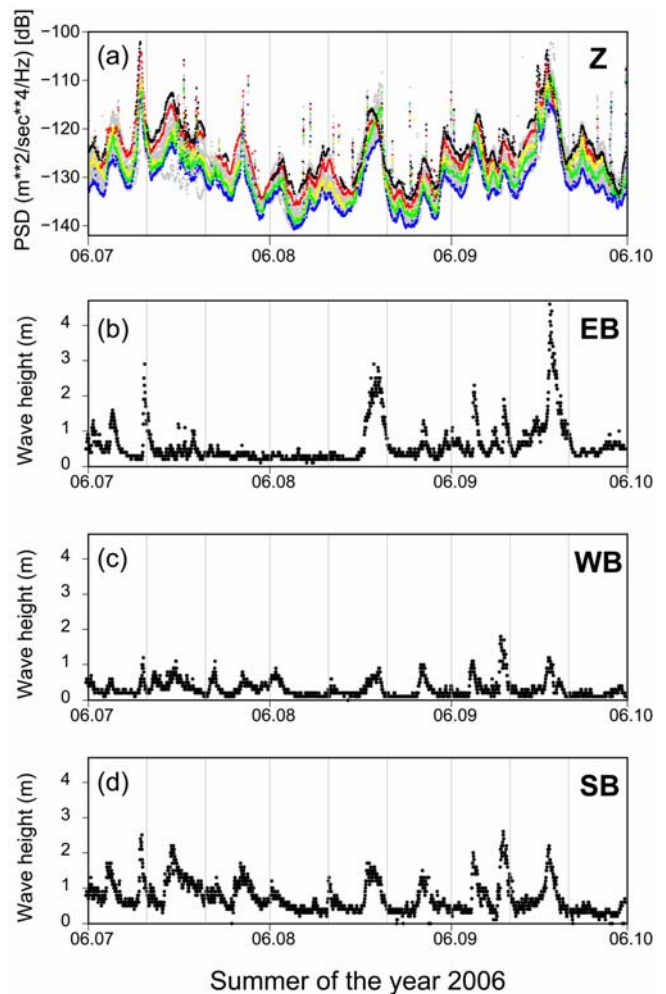

Fig. 8. Comparison of DF peaks and significant wave heights dur-ing summer 2006. (a) DF peaks of vertical component and (b–d) significant wave heights at three near-shore buoys (locations are given in Fig. 1). Gray dots represent noise levels of individual sta-tions, and black, red, yellow, green, and blue dots refer to stations JJU, BGD, GKP1, SND, and CHNB, respectively.

height (Hs) at three near-shore buoys. The buoys belong to the KMA and are located at eastern (EB), western (WB), and southwestern (SB) locations near the shore of the Korean Peninsula. Locations are given in Figure 1. The noise level in Figure 8a is evaluated every hour, and gray dots represent the noise levels of individual stations. Black, red, yellow, green, and blue dots denote the noise levels of sta-tions JJU, BGD, GKP1, SND, and CHNB, respectively. Peaks of the PSD are quite well correlated to those of the Hs. Especially around July 10, August 19, and September 18, three strong Hs peaks appear at buoys, and DF peaks are clearly observed at seismic stations. Concurrent with the occurrence of these peaks, strong Pacific typhoons Ewiniar, Shanshan, and Wukong come near the Korean Peninsula. Figure 9 shows the tracks of the Pacific typhoons from July to September 2006, obtained from the Regional Specialized
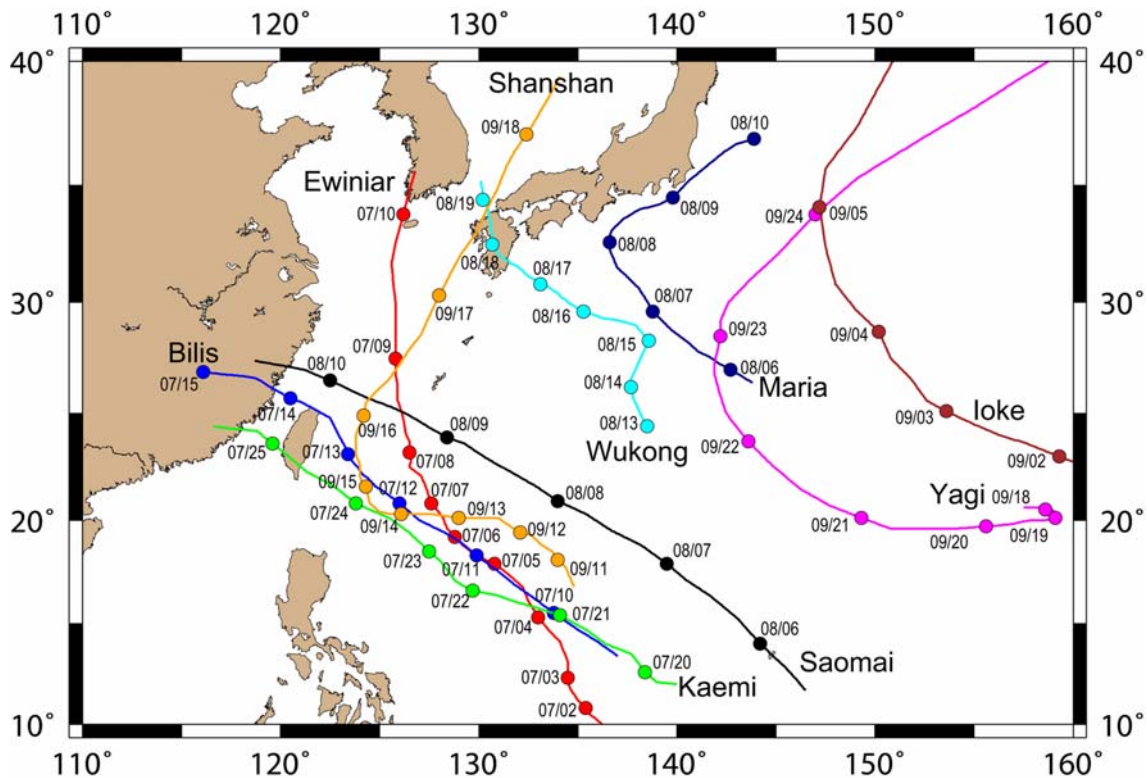
Fig. 9. Tracks of Pacific typhoons occurred from September to October, 2006.

Meteorological Center Tokyo-Typhoon Center. Other peaks also correlate with the presence of Pacific typhoons.

In general, the DF peak is observed after the ocean waves induced by the storm impacted the shoreline (Friedrich et al., 1998; Schulte-Pelkum et al., 2004; Bromirski et al., 2005; Chevrot et al., 2007). Figure 8, however, shows that most DF peaks occurred several hours in advance of Hs peaks at buoys EB and WB, while the DF and Hs peaks at buoy SB generally coincided. In addition, the amplitudes of DF peaks decrease with latitude: the DF peaks at station JJU are the highest, while those at station CHNB the lowest (Fig. 8a). Also, during winter, the DF peaks of northern stations are generally lower than those of southern stations. It is also noteworthy that DF peaks at eastern stations, such as ULL, BUS, ULJ, SND, DAG, DGY, GKP1, and KSA, are sometimes greater than those at southern stations during the passage of Pacific typhoons. These observations suggest that the generation region of most DF energy affecting South Korea is located in the sea south of the peninsula.

4. CONCLUSION

The background seismic noise of broadband stations in South Korea has been analyzed to study its characteristics and variations. Power spectral analysis (McNamara and Buland, 2004) has been applied to estimate the power spectral density for seismograms of 30 broadband stations from

2005 to 2007. In the frequency range 1–5 Hz, most stations in South Korea exhibit diurnal variations of seismic noise level and daily differences in daytime noise level, which would be strongly related to cultural activities. Cultural noise, however, has little influence on the detection capability of events over magnitude 2.0 occurring in South Korea. The DF peaks in the frequency range 0.1–0.5 Hz show systematic seasonal variations that are higher in winter than in summer. Strong DF peaks are observed in the summer when Pacific typhoons are close to the Korean Peninsula. The DF peaks occurring in advance of the Hs peaks at eastern and western buoys and the decrease of DF peaks with increasing latitude suggest that most of the DF energy likely originates in the Southern Sea of the Korean Peninsula.

REFERENCES

Aster, R. C. and Shearer, P. M., 1991, High-frequency borehole seismograms recorded in the San Jacinto fault zone, southern California. part 2. attenuation and site effects. Bulletin of the Seismological Society of America, 81, 1081–1100.

Barstow, N., Sutton, G. H. and Carter, J. A., 1989, Particle motion and pressure relationships of ocean bottom noise: 3900 m depth;

0.003 to 5 Hz. Geophysical Research Letters, 16, 1185–1188.

Bromirski, P. D., Duennebier, F. K. and Stephen, R. A., 2005, Mid-ocean microseisms. Geochemistry Geophysics Geosystems, 6, Q04009, doi:10.1029/2004GC000768.

Carter, J. A., Barstow, N., Pomeroy, P. W., Chael, E. P. and Leahy, P. J., 1991, High frequency seismic noise as a function of depth. Bulletin of the Seismological Society of America, 81, 1101–1114.

Chevrot, S., Sylvander, M., Benahmed, S., Ponsolles, C., Lefevre, J. M. and Paradis, D., 2007, Source locations of secondary microseisms in Western Europe: Evidence for both coastal and pelagic source. Journal of Geophysical Research, 112, B11301, doi:10.1029/2007JB005059.

Friedrich, A., Kruger, F. and Klinge, K., 1998, Ocean-generated microseismic noise located with the Grafenberg array. Journal of Seismology, 2, 47–64.

Gordeev, E. I., 1990, Generation of microseisms in the coastal area. Physics of the Earth and Planetary Interiors, 63, 201–208.

Hasselmann, K., 1963, A statistical analysis of the generation of microseisms. Review of Geophysics, 1, 177–209.

Haubrich, R. A. and McCamy, K., 1969, Microseisms: Coastal and pelagic sources. Review of Geophysics, 7, 539–571.

Kedar, S., Longuet-Higgins, M., Webb, F., Graham, N., Clayton, R. and Jones, C., 2008, The origin of deep ocean microseisms in the North Atlantic Ocean. Proceedings of the Royal Society A, 464, 777–793.

Longuet-Higgins, M. S., 1950, A theory of the origin of microseisms. Philosophical Transactions of the Royal Society London, Series A, 243, 1–35.

Marzorati, S. and Bindi, D., 2006, Ambient noise levels in north central Italy. Geochemistry Geophysics Geosystems, 7, Q09010, doi: 10.1029/2006GC001256.

McNamara, D. E. and Buland, R. P., 2004, Ambient noise levels in the continental United States. Bulletin of the Seismological Society of America, 94, 1517–1527.

Peterson, J., 1993, Observations and modeling of background seismic noise. U.S. Geological Survey, Open-File Report, 93–322, pages 1–95.

Rhie, J. and Romanowicz, B., 2004, Excitation of Earth's continuous free oscillations by atmosphere-ocean-seafloor coupling. Nature, 431, 552–556.

Rind, D. and Donn, W. L., 1979, Microseisms at Palisades, 2. Rayleigh wave and Love wave characteristics and the geologic control of propagation. Journal of Geophysical Research, 84, 5632–5642.

Ringdal, F. and Bungum, H., 1977, Noise level variation at NORSAR and its effect on detectability. Bulletin of the Seismological Society of America, 67, 479–492.

Schulte-Pelkum, V., Earle, P. S. and Vernon, F. L., 2004, Strong directivity of ocean-generated seismic noise. Geochemistry Geophysics Geosystems, 5, Q03004, doi:10.1029/2003GC000520.

Withers, M. M., Aster, R. C., Young, C. J. and Chael, E. P., 1996, High-frequency analysis of seismic background noise as a function of wind speed and shallow depth. Bulletin of the Seismological Society of America, 86, 1507–1515.

Young, C. J., Chael, E. P., Withers, M. M. and Aster, R. C., 1996, A comparison of the high-frequency (>1 hz) surface and subsurface noise environment at three sites in the United States. Bulletin of the Seismological Society of America, 86, 1516–1528.